



Cite this: *Chem. Commun.*, 2015, 51, 16127

Received 28th August 2015,
Accepted 15th September 2015

DOI: 10.1039/c5cc07216f

www.rsc.org/chemcomm

Fluorescent supramolecular polypseudorotaxane architectures with Ru(II)/tri(bipyridine) centers as multifunctional DNA reagents†

Wen Zhang,^a Heng-Yi Zhang,^{*ab} Yu-Hui Zhang^a and Yu Liu^{*ab}

A water-soluble supramolecular polypseudorotaxane was prepared via the host-guest interaction of cucurbit[8]uril and the Ru(bpy)₃ complex with bis-naphthalene groups. By employing the intrinsic properties of the Ru(bpy)₃ complex, the linear polypseudorotaxane can induce DNA condensation, be used as an inhibitor for DNA cleavage enzymes, and trace the translocation of DNA into 293T cells efficiently.

Supramolecular polymers have received much attention in recent years for their potential high response to stimuli, environmental adaptation, and self-repair capacity.¹ Compared with traditional polymers, supramolecular polymers can be easily and conveniently constructed through noncovalent interactions such as hydrogen bonding, π - π stacking, metal coordination, host-guest interactions, *etc.*² The main chain polypseudorotaxane is a sort of special supramolecular polymer, in which macrocyclic molecules act as both wheel components and connectors of polypseudorotaxanes.³ To obtain supramolecular polypseudorotaxanes with high molecular weight, especially at low monomer concentration, it is necessary that there exist high binding strengths among units. Cucurbit[8]uril (CB[8]), which possesses high binding constants with a variety of neutral or positively charged guests (up to 10^{15} M^{-1}),⁴ has been widely used as the connector of supramolecular architectures in aqueous solution.⁵ These studies focused primarily on the construction of supramolecular architectures, while their function research studies as biomaterials were not reported to the best of our knowledge. We recently constructed some interesting supramolecular architectures containing β -cyclodextrins and CB[6],⁶ which can induce DNA condensation, and its abilities for DNA condensation can be controlled by the number of CB[6].^{6e}

In this work, we prepared a supramolecular polypseudorotaxane *via* the host-guest interaction of CB[8] with a water-soluble Ru(bpy)₃ complex **1** (Fig. 1). We chose Ru(bpy)₃ as the metal complex because of some of its unique characteristics. (1) The big Ru(bpy)₃ complex⁷ can suppress the formation of cyclic species; (2) this complex is stable and water-soluble, which can increase the solubility of CB[8] in water through host-guest interactions; (3) it is a multifunctional group as photocatalysts, building blocks for conducting polymers, DNA probes, or fluorophores for electrochemoluminescence.⁸ As a result, combination of the biocompatibility⁹ and low toxicity¹⁰ of CB[8] and the DNA-interaction properties of polypyridine-ruthenium complexes

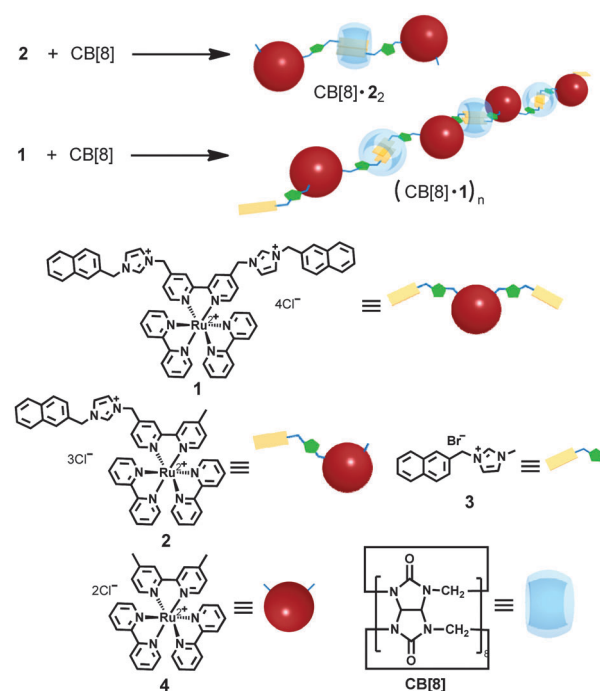


Fig. 1 Formation of supramolecular complex CB[8]·2 and supramolecular polypseudorotaxane (CB[8]·1)_n, and structural illustration of CB[8], Ru(bpy)₃ complexes **1**, **2**, **4**, and control compound **3**.

^a Department of Chemistry, State Key Laboratory of Elemento-Organic Chemistry, Nankai University, Collaborative Innovation Center of Chemical Science and Engineering, Tianjin 300071, P. R. China. E-mail: hyzhang@nankai.edu.cn

^b Collaborative Innovation Center of Chemical Science and Engineering, Nankai University, Tianjin 300071, P. R. China. E-mail: yuliu@nankai.edu.cn

† Electronic supplementary information (ESI) available: Synthesis and characterization of **1**, **2**, **3** and **4**, and experimental details. See DOI: 10.1039/c5cc07216f

would facilitate the water-soluble supramolecular polypseudorotaxane being a multifunctional biomaterial. Using UV-vis/fluorescence spectroscopy, NMR spectroscopy, diffusion-ordered NMR spectroscopy (DOSY), dynamic laser scattering (DLS), atomic force microscopy (AFM), agarose gel electrophoresis, and confocal laser scanning microscopy, we will demonstrate the formation of the supramolecular polypseudorotaxane and its abilities to induce the aggregation of DNA, inhibit the DNA cleavage enzyme, and trace the translocation of DNA into cells.

Starting from 4,4'-dimethyl-2,2'-bipyridine (Scheme S1, ESI[†]), after oxidation, esterification, reduction and substitution reactions as previously described in the literature,¹¹ we synthesized 4,4'-bis(bromomethyl)-2,2'-bipyridine. Followed by reaction with 1-(naphthalen-2-ylmethyl)-1*H*-imidazole,¹² bipyridine imidazolium was obtained in 92% yield. After complexation with Ru(bpy)₂Cl₂·2H₂O and ion metathesis procedures, complex **1** (85% yield) was obtained as a dark red solid. Using a similar synthetic strategy, we synthesized complex **2** in 80% yield. The supramolecular polypseudorotaxane was constructed by the complexation of **1** with CB[8] in aqueous solution. A control supramolecular dimer was also formed by the complexation of **2** with CB[8] (Fig. 1).

UV-vis spectroscopy and fluorescence spectroscopy were employed to collect information on the binding model between **1–3** and CB[8], respectively. For compound **3**, there is an absorption band at 275 nm in its UV-vis spectrum. Adding 0.5 eq. CB[8] into its aqueous solution caused a decrease of the absorption of the naphthalene (Fig. S1a, ESI[†]), indicating that naphthalene moieties are encapsulated in the cavity of CB[8].¹³ For complexes **1** and **2**, there are similar absorption bands in the presence of CB[8] besides the typical metal-to-ligand charge-transfer (MLCT) band peak at around 450 nm (Fig. S1b and c, ESI[†]), which suggests the existence of Ru(bpy)₃ moieties. Fluorescence spectroscopy experiments will provide a further insight into the types of interactions between each of the guest molecules in the supramolecular architectures. Fig. S1d (ESI[†]) shows fluorescence spectra for the titration of CB[8] into an aqueous solution of **3**. Upon the addition of CB[8], the emission peak at 335 nm was significantly quenched, and simultaneously, a new emission band emerged at 405 nm with an isoabsorptive point at 370 nm. This observation suggests that the naphthalene moieties are π–π stacked inside CB[8]'s cavity, forming CB[8] enhanced π–π complexes.¹⁴ Surprisingly, when CB[8] was added into the aqueous solution of **1** or **2**, the emission peak at 400–450 nm did not increase, but be quenched (Fig. 2). In the meanwhile, the emission peak at 650 nm was enhanced significantly. One reasonable explanation is the occurrence of a resonance energy transfer (RET), because the emission spectrum of the π–π complexes between two naphthalene moieties as donors overlaps the absorption spectrum of **1** or **2** as the acceptor. Therefore, these fluorescence experiments also confirm that the naphthalene moieties of **1** and **2** are π–π stacked inside CB[8]'s cavity, as illustrated in Fig. 1.

DOSY, DLS, and AFM were subsequently employed to identify the formation, the size, and the morphology of the supramolecular polypseudorotaxanes based on the host–guest interaction of **1** with CB[8]. As can be seen in Table 1, the average diffusion coefficients of compounds **1**, **2** and CB[8]¹⁵ were $2.94 \times 10^{-10} \text{ m}^2 \text{ s}^{-1}$,

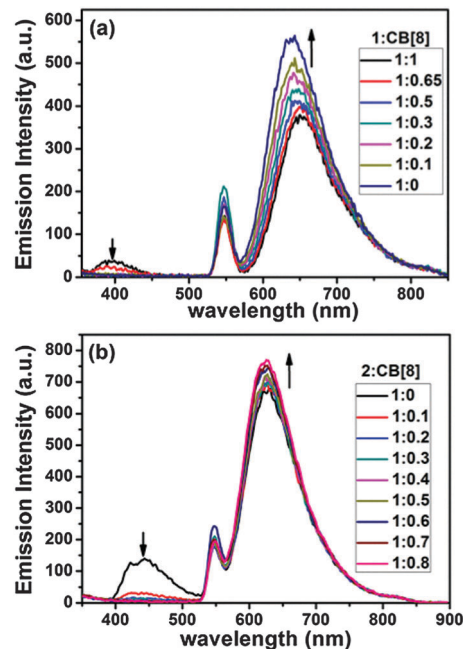


Fig. 2 (a) Emission spectra for the titration of CB[8] into an aqueous solution of **1** ($1 \times 10^{-5} \text{ M}$); (b) emission spectra for the titration of CB[8] into an aqueous solution of **2** ($1 \times 10^{-5} \text{ M}$).

$3.17 \times 10^{-10} \text{ m}^2 \text{ s}^{-1}$ and $2.93 \times 10^{-10} \text{ m}^2 \text{ s}^{-1}$, respectively. For the CB[8]-**2** solution, the Davg value was $1.94 \times 10^{-10} \text{ m}^2 \text{ s}^{-1}$, while the NMR signals of (CB[8]-**1**)_n show a single diffusion coefficient with a smaller value of $1.07 \times 10^{-10} \text{ m}^2 \text{ s}^{-1}$. By simplistically assuming all assemblies as hydrodynamically spherical,¹⁶ the average degree of supramolecular polymerization can be estimated from the obtained diffusion coefficients according to the Stokes–Einstein equation ($D = k_B T / (6\pi\eta R)$). The average size of the dimer CB[8]-**2**₂ complexes is 3.4 times of CB[8], which is consistent with theoretical predictions. While (CB[8]-**1**)_n complexes are 20.6 times larger than CB[8], which implies that large-size supramolecular polypseudorotaxanes have been formed indeed. The morphology of the supramolecular polypseudorotaxane was investigated by AFM measurement (Fig. S6, ESI[†]). As expected, 1D linear objects were observed, and the height of these 1D nanostructures was 1.57 nm, which is identical to the outside diameter of CB[8] (1.75 nm). DLS experiments show a broad peak (Fig. S7, ESI[†]) at 223 nm, which further indicates the formation of a variety of highly polymerized supramolecular assemblies.

The DNA interaction abilities of the polypseudorotaxane were investigated by means of agarose gel electrophoresis. The gel retardation assay was performed using polypseudorotaxane

Table 1 Diffusion coefficients (*D*) obtained from DOSY measurements

Complex	Diffusion coefficient ($\text{m}^2 \text{ s}^{-1}$)	$V_{\text{complex}}/V_{\text{CB[8]}}$
CB[8]	2.93×10^{-10}	1
1	2.94×10^{-10}	0.99
1 + CB[8]	1.07×10^{-10}	20.6
2	3.17×10^{-10}	0.79
2 + CB[8]	1.94×10^{-10}	3.4

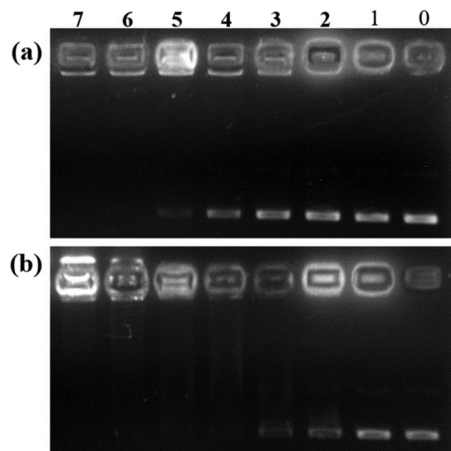


Fig. 3 Agarose gel electrophoresis assay to investigate the DNA condensation induced by supramolecular polypseudorotaxane (a) **1**/CB[8] (1:1) and (b) **2**/CB[8] (2:1) dimer: lane 0, DNA alone; lanes 1–7, DNA + polypseudorotaxane or dimer. The DNA concentration is $15 \text{ ng } \mu\text{L}^{-1}$. The different concentrations of supramolecular polypseudorotaxane from lane 1 to lane 7 were 0.5, 1, 2, 3, 4, 5, 7.5 μM , supramolecular dimer from lane 1 to lane 7 were 5, 10, 25, 50, 100, 150, 200 μM , respectively.

(CB[8]-**1**)_n and dimer CB[8]-**2**₂, respectively. As can be seen from Fig. 3, with the increase of the concentration of polypseudorotaxane/dimer, the retardation of DNA was clearly observed in the gel loading wells. When the concentration of Ru(bpy)₃ complex **1** in the polypseudorotaxane (CB[8]-**1**)_n is 5 μM , DNA could be condensed completely. For CB[8]-**2**₂, this value is 200 μM until DNA is condensed completely. That is to say, the DNA-condensing efficiency of the polypseudorotaxane is amplified 40 times compared with the dimer. To further illustrate the superiority of the polypseudorotaxane in the condensation of DNA, we also carried out the control experiments with **4**, **2**, **1**, CB[8]-**2**₂ and (CB[8]-**1**)_n as DNA flocculants at the same Ru(bpy)₃ complex concentration (10 μM) (Fig. S8, ESI[†]). The result shows that only the polypseudorotaxane (CB[8]-**1**)_n can condense DNA completely.

More intuitive information about DNA aggregation was obtained from AFM. As shown in Fig. 4, the free supercoiled pBR322 DNA was loose and wirelike on the mica surface (Fig. 4a), whereas, in the presence of supramolecular polypseudorotaxane

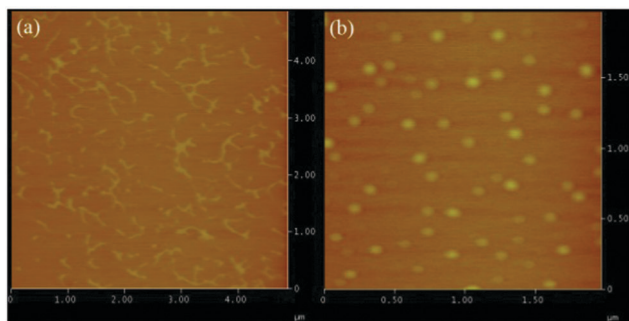


Fig. 4 AFM images showing the condensation effect of the polypseudorotaxane. (a) Free pBR322 DNA ($1 \text{ ng } \mu\text{L}^{-1}$) and (b) DNA condensation induced by linear polypseudorotaxane ($37 \text{ ng } \mu\text{L}^{-1}$).

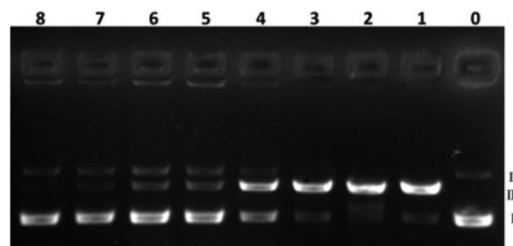


Fig. 5 Agarose gel electrophoresis assay to investigate the inhibition ability of the polypseudorotaxane against HindIII using pBR322 DNA ($21 \text{ ng } \mu\text{L}^{-1}$). Lane 0, DNA alone; lane 1, DNA + HindIII; lanes 2–8, DNA + HindIII + polypseudorotaxane (polypseudorotaxane = 1.25, 5, 10, 18.6, 37.2, 45 and $75 \text{ ng } \mu\text{L}^{-1}$, i.e., 0.5, 2, 4, 7.5, 15, 20, and 30 μM from lane 2 to lane 8). All of the samples were incubated in the dark for 1 h. Samples 1–8 were then incubated with HindIII for 15 min, according to the protocols recommended by the supplier.

the originally loose DNA lines turned to be tightly compacted particles (Fig. 4b).

HindIII, derived from *Haemophilus influenzae*, recognizing the palindromic DNA sequence 5'-AAGCTT-3'/3'-TTCGAA-5', is a common restriction enzyme *in vivo*, and can specifically cleave closed supercoiled DNA (form I) and nicked circular DNA (form II) into linear DNA (form III).¹⁷ Herein, we examined the inhibition ability of the supramolecular polypseudorotaxane against HindIII. Agarose gel electrophoresis assay of pBR322 DNA at various (CB[8]-**1**)_n/DNA mass ratios in the presence of HindIII was carried out, with parent pBR322 DNA as a control sample. As can be seen from Fig. 5, almost all of form I and form II DNA are cleaved into form III DNA in the absence of this polypseudorotaxane (lane 1). With the increase of the (CB[8]-**1**)_n/DNA mass ratio, the activity of the DNA restriction enzyme HindIII is gradually inhibited. When the (CB[8]-**1**)_n/DNA mass ratio reaches 3.6, it is inhibited thoroughly. Here, we proposed the possible reason for the efficient inhibition of the polypseudorotaxane against HindIII as the aggregation of DNA. It is well known that HindIII could specifically recognize the palindromic DNA sequence 5'-AAGCTT-3'/3'-TTCGAA-5'. When parent DNA presents as loose wirelike structure, the specific sequence is available to HindIII. Upon the addition of the supramolecular polypseudorotaxane, loose DNA was compacted and the specific sequences were shielded consequently. Hence, the cleavage ability of HindIII was weakened effectively.

Considering the good fluorescence properties of ruthenium complexes, we wondered whether this supramolecular polypseudorotaxane could be used as a DNA translocation marker as well as a carrier into cells. Firstly, we conducted cytotoxicity assay (Fig. S21, ESI[†]), and the result shows that the cell survival rate reached 89.29% when the concentration of Ru(bpy)₃ complex **1** in (CB[8]-**1**)_n polypseudorotaxane is 0.8 mM, which indicates its low cytotoxicity. In the following DNA translocation experiments, the polypseudorotaxane and pBR322 DNA were mixed and kept in the dark for 1 h at 25 °C, and then the (CB[8]-**1**)_n/DNA mixture was added into routinely cultured 293T cells. After 6 h, the DNA translocation mark efficiency was monitored by confocal fluorescence imaging. As shown in Fig. S22a (ESI[†]), almost all the cells treated with (CB[8]-**1**)_n polypseudorotaxane exhibited

apparent red fluorescence, and the luminescent $(\text{CB}[8]\cdot\text{1})_n/\text{DNA}$ system is located mainly in the cytoplasm. This observation suggests a quite high DNA translocation efficiency of the polypseudorotaxane. In the control experiments under the same conditions, the confocal fluorescence imaging of the 293T cells presents no obvious red fluorescence in the presence of the polypseudorotaxane barely (Fig. S22b, ESI[†]). These results demonstrate that the polypseudorotaxane can be used as not only a gene carrier but also an efficient luminescent marker for the DNA translocation.

In conclusion, we have constructed a water-soluble multi-functional supramolecular polypseudorotaxane through $\text{CB}[8]$ -enhanced π - π interactions and exploited its biological functions. The results obtained demonstrate that this linear fluorescent supramolecular polypseudorotaxane not only exhibits better condensation abilities toward DNA than those short species such as monomer **4** and dimer $\text{CB}[8]\cdot\text{2}$, but also could inhibit the activity of DNA restriction enzyme. Owing to its good fluorescence properties, the polypseudorotaxane was also successfully used to mark the translocation of DNA into cells. Owing to these advantages, this supramolecular polypseudorotaxane is expected to have potential applications in pharmaceutical chemistry and biological technology fields.

We acknowledge the 973 Program (2011CB932500 and 2015CB856500) and the NNSFC (No. 21372128 and 91227107) for financial support.

Notes and references

- (a) T. F. A. d. Greef and E. W. Meijer, *Nature*, 2008, **453**, 171–173; (b) M. Burnworth, L. Tang, J. R. Kumpfer, A. J. Duncan, F. L. Beyer, G. L. Fiore, S. J. Rowan and C. Weder, *Nature*, 2011, **472**, 334–337; (c) T. Aida, E. W. Meijer and S. I. Stupp, *Science*, 2012, **335**, 813–817; (d) X. Ma and H. Tian, *Acc. Chem. Res.*, 2014, **47**, 1971–1981; (e) J. del Barrio, P. N. Horton, D. Lairez, G. O. Lloyd, C. Toprakcioglu and O. A. Scherman, *J. Am. Chem. Soc.*, 2013, **135**, 11760–11763; (f) E. A. Appel, X. J. Loh, S. T. Jones, F. Biedermann, C. A. Dreiss and O. A. Scherman, *J. Am. Chem. Soc.*, 2012, **134**, 11767–11773.
- (a) L. Yang, X. Tan, Z. Wang and X. Zhang, *Chem. Rev.*, 2015, **115**, 7196–7239; (b) S. Dong, B. Zheng, F. Wang and F. Huang, *Acc. Chem. Res.*, 2014, **47**, 1982–1994; (c) N. Song, D. X. Chen, M. C. Xia, X. L. Qiu, K. Ma, B. Xu, W. Tian and Y. W. Yang, *Chem. Commun.*, 2015, **51**, 5526–5529; (d) N. Song, D. X. Chen, Y. C. Qiu, X. Y. Yang, B. Xu, W. Tian and Y. W. Yang, *Chem. Commun.*, 2014, **50**, 8231–8234; (e) E. A. Appel, F. Biedermann, U. Rauwald, S. T. Jones, J. M. Zayed and O. A. Scherman, *J. Am. Chem. Soc.*, 2010, **132**, 14251–14260.
- (a) M. Arunachalam and H. W. Gibson, *Prog. Polym. Sci.*, 2014, **39**, 1043–1073; (b) Y. Liu, S. H. Song, Y. Chen, Y. L. Zhao and Y. W. Yang, *Chem. Commun.*, 2005, 1702–1704.
- M. V. Rekharsky, T. Mori, C. Yang, Y. H. Ko, N. Selvapalam, H. Kim, D. Sobransingh, A. E. Kaifer, S. Liu, L. Isaacs, W. Chen, S. Moghaddam, M. K. Gilson, K. Kim and Y. Inoue, *Proc. Natl. Acad. Sci. U. S. A.*, 2007, **104**, 20737–20742.
- (a) L. Brunsveld, B. J. B. Folmer, E. W. Meijer and R. P. Sijbesma, *Chem. Rev.*, 2001, **101**, 4071–4098; (b) H.-J. Kim, J. Heo, W. S. Jeon, E. Lee, J. Kim, S. Sakamoto, K. Yamaguchi and K. Kim, *Angew. Chem., Int. Ed.*, 2001, **40**, 1526–1529; (c) Y. Liu, H. Yang, Z. Wang and X. Zhang, *Chem. – Asian J.*, 2013, **8**, 1626–1632; (d) F. Biedermann, V. D. Uzunova, O. A. Scherman, W. M. Nau and A. De Simone, *J. Am. Chem. Soc.*, 2012, **134**, 15318–15323; (e) U. Rauwald and O. A. Scherman, *Angew. Chem., Int. Ed.*, 2008, **47**, 3950–3953.
- (a) J. Zhao, Y. M. Zhang, H. L. Sun, X. Y. Chang and Y. Liu, *Chem. – Eur. J.*, 2014, **20**, 15108–15115; (b) Q. Wang, Y. Chen and Y. Liu, *Polym. Chem.*, 2013, **4**, 4192–4198; (c) L. Li, H. Y. Zhang, J. Zhao, N. Li and Y. Liu, *Chem. – Eur. J.*, 2013, **19**, 6498–6506; (d) H. Qian, D. S. Guo and Y. Liu, *Chem. – Eur. J.*, 2012, **18**, 5087–5095; (e) C.-F. Ke, S. Hou, H.-Y. Zhang, Y. Liu, K. Yang and X.-Z. Feng, *Chem. Commun.*, 2007, 3374–3376.
- E. E. Pérez-Cordero, C. Campana and L. Echegoyen, *Angew. Chem., Int. Ed.*, 1997, **36**, 137–140.
- (a) T. P. Yoon, M. A. Ischay and J. N. Du, *Nat. Chem.*, 2010, **2**, 527–532; (b) S. Zhang, Y. Ding and H. Wei, *Molecules*, 2014, **19**, 11933–11987; (c) W. J. Youngblood, S.-H. A. Lee, K. Maeda and T. E. Mallouk, *Acc. Chem. Res.*, 2009, **42**, 1966–1973; (d) H.-J. Li, S. Han, L.-Z. Hu and G.-B. Xu, *Chin. J. Anal. Chem.*, 2009, **37**, 1557–1565.
- (a) G. Hettiarachchi, D. Nguyen, J. Wu, D. Lucas, D. Ma, L. Isaacs and V. Briken, *PLoS One*, 2010, **5**, e10514; (b) Q. L. Li, Y. Sun, Y. L. Sun, J. Wen, Y. Zhou, Q. M. Bing, L. D. Isaacs, Y. Jin, H. Gao and Y. W. Yang, *Chem. Mater.*, 2014, **26**, 6418–6431.
- (a) N. J. Wheate, D. P. Buck, A. I. Day and J. G. Collins, *Dalton Trans.*, 2006, 451–458; (b) V. D. Uzunova, C. Cullinane, K. Brix, W. M. Nau and A. I. Day, *Org. Biomol. Chem.*, 2010, **8**, 2037–2042.
- I. Gillaizeau-Gauthier, F. Odobel, M. Alebbi, R. Argazzi, E. Costa, C. A. Bignozzi, P. Qu and G. J. Meyer, *Inorg. Chem.*, 2001, **40**, 6073–6079.
- N. Matsunaga, T. Kaku, F. Itoh, T. Tanaka, T. Hara, H. Miki, M. Iwasaki, T. Aono, M. Yamaoka, M. Kusaka and A. Tasaka, *Bioorg. Med. Chem.*, 2004, **12**, 2251–2273.
- Y. L. Jiang, X. Gao, G. Zhou, A. Patel and A. Javer, *J. Org. Chem.*, 2010, **75**, 324–333.
- D. Jiao, F. Biedermann, F. Tian and O. A. Scherman, *J. Am. Chem. Soc.*, 2010, **132**, 15734–15743.
- Y. Liu, R. Fang, X. Tan, Z. Wang and X. Zhang, *Chem. – Eur. J.*, 2012, **18**, 15650–15654.
- R. Schmidt, M. Stolte, M. Grüne and F. Würthner, *Macromolecules*, 2011, **44**, 3766–3776.
- D. H. Tang, S. Ando, Y. Takasaki and J. Tadano, *Protein Eng.*, 2000, **13**, 283–289.